Journal of Chromatography, 214 (1981) 269–282
Elsevier Scientific Publishing Company, Amsterdam — Printed in The Netherlands

CHROM. 13,976

GAS–SOLID CHROMATOGRAPHY OF ETHANE ON ACTIVATED CARBON AT 25 C

JAN-CHAN HUANG, ROBERT FORSYTHE and RICHARD MADEY*
Department of Physics, Kent State University, Kent, OH 44242 (U.S.A.)
(First received March 10th, 1981; revised manuscript received May 7th, 1981)

SUMMARY

The adsorption and diffusion of ethane in a chromatographic column packed with activated carbon were investigated for different concentrations and flow-rates. The adsorption isotherm of ethane can be represented by a three-parameter equation. The experimental data and theoretical asymptotic concentration profiles agree at high inlet concentrations and deviate at low inlet concentrations. The longitudinal diffusion coefficients were extracted from fitting the experimental data. Analytic criteria presented here for achieving an asymptotic concentration profile predict that the best result occurs at the flow-rate corresponding to the minimum of the height equivalent to a theoretical plate.

INTRODUCTION

Developments in gas–solid chromatography (GSC) progress less rapidly than in gas–liquid chromatography (GLC) because of the mathematical difficulty associated with a non-linear isotherm for gas–solid equilibrium, which is usually observed even at very low concentrations[1]. The analysis of GSC usually assumes that there is no variation of the gas-flow velocity in the radial direction and that longitudinal diffusion is negligible. These assumptions avoid the difficulty associated with a non-linear isotherm by permitting a first-order partial-differential equation which can be solved formally by a suitable transform of variables[2,3]. When longitudinal diffusion is taken into consideration, the differential equation is generally too complicated to solve analytically except for certain simple isotherms (*e.g.*, linear[4] or Langmuir[5]); however, some of the important physical properties such as adsorption capacities and diffusion coefficients can still be determined from transmission data for a step-function input provided the concentration has reached an asymptotic concentration profile.

After an adsorbate traverses a sufficiently long column, the adsorbate concentration reaches an asymptotic form called the asymptotic concentration profile. An asymptotic concentration profile occurs for a step-increase in the concentration of an adsorbate that exhibits a convex isotherm (*e.g.*, Langmuir or type I BET) and also for a step-decrease in the concentration of an adsorbate with a concave isotherm such as

0021-9673/81/0000–0000/$02.50

type III BET. An asymptotic concentration profile results when the effect of diffusion is offset by the effect of the curvature of the isotherm. For an observer moving with the average migration speed of the adsorbate, the concentration profile is independent of time. An asymptotic concentration profile can be measured as a function of the longitudinal coordinate by an observer moving along with the adsorbate or as a function of time by a laboratory observer. The possibility of approaching an asymptotic concentration profile was first noted by Sillen and Ekedahl[6]. Later Lapidus and Rosen[7] studied the asymptotic concentration profile of an ion-exchange column; Lightfoot[8] gave more quantitative mathematical discussions for an equilibrium system with longitudinal diffusion; and Acrivos[9] discussed a system with external mass-transfer resistance. Reports of experimental work on asymptotic concentration profiles are rare in the literature in comparison with theoretical discussions. In this paper, we present experimental results for the transmission of ethane on activated carbon at 25°C; calculate the adsorption capacity for ethane at different inlet concentrations; and compare transmission data with theoretical curves. Transmission is the ratio of the outlet concentration to the inlet concentration.

THEORY

For isothermal adsorption of a trace component in a constant carrier-gas flow, the equation for the gas-phase adsorbate concentration C can be written as[4,8,9]:

$$\frac{\partial}{\partial t}[\varepsilon C + (1 - \varepsilon)\, q] = D\frac{\partial^2 C}{\partial Z^2} - u\frac{\partial C}{\partial Z} \tag{1}$$

The initial and boundary conditions for an initially desorbed column are:

$$C(Z, 0) = 0 \tag{2}$$

$$q(Z, 0) = 0 \tag{3}$$

$$C(0, t) = C_0 \tag{4}$$

$$C(\infty, t) = 0 \tag{5a}$$

$$q(\infty, t) = 0 \tag{5b}$$

The symbol q is the solid-phase concentration of the adsorbate, ε is the void fraction in the packed column, u is the superficial flow velocity of the gas mixture, and D is the longitudinal diffusion coefficient. We used an infinite column length for the boundary condition in eqns. 5a and 5b because the asymptotic concentration profile can be attained only after a sufficiently long distance.

Let us introduce a new moving coordinate variable X defined as[8]:

$$X \equiv \frac{u}{D}\left[Z - \frac{C_0\, ut}{\varepsilon C_0 + (1 - \varepsilon)\, q_0}\right] \tag{6}$$

[where $q_0 = q\ (0, t)$]. For an asymptotic concentration profile, eqn. 1 becomes

$$\frac{d^2 C}{dX^2} - \frac{d}{dX} \frac{Cq_0 - qC_0}{\frac{\varepsilon C_0}{1 - \varepsilon} + q_0} = 0 \tag{7}$$

Note that the concentration C is a function of X only. Eqn. 7 can then be integrated to yield

$$\frac{dC}{dX} - \frac{Cq_0 - qC_0}{\frac{\varepsilon C_0}{1 - \varepsilon} + q_0} = 0 \tag{8}$$

where we used eqns. 5a and 5b and the fact that the slope $\left(\frac{dC}{dX}\right)_{C=0}$ of the asymptotic concentration profile at the leading-edge ($C \equiv 0$) is zero. The integration of eqn. 8 gives the formal solution for the asymptotic concentration profile[8]:

$$\frac{t_2 - t_1}{\tau} = \frac{X_1 - X_2}{\frac{\varepsilon C_0}{(1 - \varepsilon)\, q_0} + 1} = \int_{C_1/C_0}^{C_2/C_0} \frac{d\ C/C_0}{q/q_0 - C/C_0} \tag{9}$$

where the definition of the time-constant τ is

$$\tau \equiv \frac{D\,[C_0\,\varepsilon + q_0\,(1 - \varepsilon)]^2}{q_0\,C_0\,u^2\,(1 - \varepsilon)} \tag{10}$$

The derivation of eqn. 9 does not depend on any specific relation between C and q. The only prerequisite is that the integral converges. Note that for the case of a convex isotherm, the integral has a negative value and the asymptotic concentration occurs for the desorption profile where C decreases with increasing values of the time coordinate t/τ. For a linear isotherm (*viz.*, q/C = constant), the integral diverges. Thus, eqn. 9 indicates a well-known fact that the profile of a linear-isotherm system diffuses continuously without forming an asymptotic concentration profile[10,11]; moreover, it does not demand an equilibrium relation between the gas-phase and the solid-phase. When the non-equilibrium relation prevails, both C and q still have asymptotic concentration profiles; but another equation is needed to obtain an expression for C and q as a function of the coordinate X. Garg and Ruthven[12] studied the non-equilibrium case for a Langmuir isotherm, which requires extensive numerical calculations. Since the flow-rates of the gas mixtures in this study were low, we treat here only the equilibrium relation between the gas and solid-phases[11]; furthermore, the approximations leading to eqn. 1 do not warrant introducing the intricate mass-transfer resistances in this study.

EXPERIMENTAL

The flow system and experimental procedures were described earlier[13]. The chromatographic column was a stainless-steel cylinder, 10 cm × 0.46 cm I.D., which

contained 0.588 gram of Columbia 4LXC 12/28 activated carbon (Union Carbide, New York, NY, U.S.A.). The carbon has intrinsic density 1.56 g/cm^3 and pore volume 0.51 cm^3/g. The composition of inlet ethane was controlled by two valves which separately adjusted the flow-rates of the pure helium and the calibrated ethane–helium mixture. Two calibrated ethane–helium mixtures were prepared by Matheson Gas Products (East Rutherford, NJ, U.S.A.) with nominal ethane concentrations of 500 and 10,000 ppm. The flow of each gas and the total flow-rate can be controlled to within an accuracy of $\pm 0.5\%$. The system pressure in the chromatographic column varied between 740 and 760 mmHg, but the pressure differences between the inlet and the outlet were always less than 10 mmHg. The activated carbon column was immersed in a two-layer water-bath which controlled the temperature at 25°C to within ± 0.02°C. The concentration of ethane at the outlet of the adsorber bed was measured at regular time intervals by a Varian 3700 gas chromatograph and a Spectra-Physics Minigrator. Transmissions at the outlet were corrected for detector non-ideality.

RESULTS AND DISCUSSION

Determination of the isotherm

The time-dependent transmission of ethane was measured for eight concentrations at various flow velocities; in addition, the transmission of the nominal 500 ppm mixture was measured at three flow velocities. Since the data show a regular trend, we list only four concentrations in Table I. The solid-phase concentration q_0 was calculated from the mass-balance equation

$$q_0 (1 - \varepsilon) L + C_0 \varepsilon L = u C_0 \int_0^{\infty} \left(1 - \frac{C}{C_0}\right) dt \equiv u C_0 t_p \tag{11}$$

The propagation time t_p, which represents the average retention time of the adsorbate, was calculated from the transmission data by numerical integration. In eqn. 11, the integration term represents the adsorbate retained in the packed bed, while the first term and the second term of the left-hand side represent the adsorbate in the solid-phase and the gas-phase, respectively. From eqn. 11, the adsorption capacity K_0 is calculated as

$$K_0 \equiv \frac{q_0}{C_0} = \frac{1}{1 - \varepsilon}\left(\frac{u t_p}{L} - \varepsilon\right) \tag{12}$$

Gas-phase concentrations, solid-phase concentrations, and dimensionless adsorption capacities are listed in Table II for each run.

Fig. 1 is a plot of the relation between the solid-phase concentration and the gas-phase concentration. It is seen clearly that the solid-phase concentration increases with a decreasing slope when the gas-phase concentration increases. The gas–solid equilibrium relation does not follow either the Freundlich isotherm, which predicts a straight line on a logarithmic plot, or the Langmuir isotherm, which is shown as a dashed line fitted to the data for the two highest concentrations. In general, the Langmuir equation predicts a saturation of the solid-phase concentration at high gas-phase concentrations,and a proportional relation between gas- and solid-phase con-

TABLE I

TRANSMISSION *VERSUS* TIME OF FOUR DIFFERENT CONCENTRATIONS OF ETHANE IN A HELIUM CARRIER GAS FLOWING THROUGH AN ACTIVATED-CARBON ABSORBER BED AT 25°C

C_0 (10^{-8} moles/cm^3)							
39.2		10.1		1.98		0.47	
Run No.							
1		3		5B		7	
Time (sec)	Transmission	Time (sec)	Transmission	Time (sec)	Transmission	Time (sec)	Transmission
1920	0.00443	2120	0.00788	1670	0.00547	1650	0.00647
2020	0.0128	2220	0.0112	1770	0.0127	1770	0.0212
2120	0.0843	2320	0.0273	1870	0.0319	1890	0.0564
2220	0.349	2420	0.0721	1970	0.0732	2010	0.121
2320	0.668	2520	0.172	2070	0.150	2130	0.228
2420	0.856	2620	0.334	2170	0.267	2250	0.366
2520	0.940	2720	0.522	2270	0.415	2370	0.519
2620	0.975	2820	0.689	2370	0.569	2490	0.663
2720	0.989	2920	0.755	2470	0.705	2610	0.779
2820	0.9949	3020	0.888	2570	0.810	2730	0.864
2920	0.9978	3120	0.936	2670	0.883	2850	0.920
3020	0.9988	3220	0.964	2770	0.930	2970	0.956
		3320	0.980	2870	0.960	3090	0.975
		3420	0.988	2970	0.977	3210	0.987
		3520	0.9934	3070	0.990	3330	0.9920
		3620	0.99618			3550	0.9954

TABLE II

ETHANE CONCENTRATION IN THE GAS AND SOLID PHASES, THE DIMENSIONLESS ADSORPTION CAPACITY AND THE FLOW-RATE FOR EACH RUN

Run No.	Mole fraction of ethane (ppm)	Superficial flow-rate, u (cm/sec)	Gas-phase concentration, C_0 (10^{-9} mole/cm^3)	Solid-phase concentration, q_0 (10^{-5} mole/cm^3)	Adsorption capacity, K
1	9830	1.50	392	58.6	1500
2	5186	1.52	210	36.8	1760
3	2478	1.76	101	21.3	2100
4	1160	2.22	47.5	11.3	2380
5A	495	1.47	20.2	5.14	2550
5B	495	2.51	19.8	5.10	2580
5C	495	4.63	19.8	5.18	2620
6	229	2.52	9.29	2.58	2780
7	115	2.78	4.67	1.35	2900
8	44.7	3.05	1.82	0.54	2960

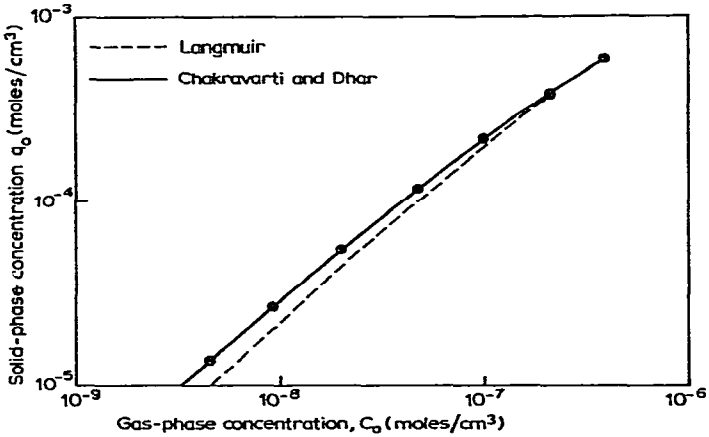

Fig. 1. The solid-phase concentration *versus* the gas-phase concentration. Circles are experimental results. The solid line is the isotherm of Chakravarti and Dhar[16]. The dashed line is the Langmuir equation fitted through the two points with the highest concentration.

centrations at low gas-phase concentrations. Our results on a logarithmic plot show a straight-line relation with a slope less than unity at low concentrations and a slightly convex curve at high concentrations. Similar experimental results were reported[14] in studies of the surface adsorption on non-polar solids at low concentrations of various gases; most of the isotherms[15], which were suggested to fit these data, contain the logarithm of the partial pressure of the adsorbate. Since the adsorbate concentration is zero initially, the inclusion of a logarithmic function causes a mathematical difficulty; therefore, to simplify the calculation we adopted the three-parameter isotherm of Chakravarti and Dhar[16]:

$$\frac{q_0}{q_0^s} = \frac{(K_m C_0)^v}{1 + (K_m C_0)^v} \tag{13}$$

Here q_0^s is the solid-phase concentration for monolayer coverage, and K_m and v are constants. Eqn. 13 will simplify to the Freundlich equation when $K_m C_0$ is very small. Also it simplifies to the Langmuir equation when $v = 1$.

The three parameters of eqn. 13 can be determined from experimental data. In order to calculate the parameters, we rewrite eqn. 13 as:

$$\log \frac{q_0}{q_0^s - q_0} - v \log K_m - v \log C_0 = 0 \tag{14}$$

The simultaneous determination of the three parameters (*viz.*, q_0^s, v, and K_m) requires a complicated calculation; however, the unique expression of eqn. 14 allows us to use a simple linear least-squares method to determine v and K_m provided q_0^s is known. In this method, we assume a value for q_0^s and calculate the best values for v and K_m for the assumed q_0^s. Also for each assumed q_0^s, we calculate the sum of the squares of the errors in the linear least-squares calculation. In Fig. 2, we plot the sum of squares of the errors for the assumed values of q_0^s ranging from $1.5 \cdot 10^{-3}$ to $2.5 \cdot 10^{-3}$ mole/cm^3.

The best value for q_0^* corresponding to the smallest error is $1.9 \cdot 10^{-3}$ mole/cm^3; according to this value, v and K_m are 0.927 and $1.06 \cdot 10^6$ cm^3/mole, respectively. The solid line in Fig. 1 is the calculated isotherm based on the above parameters.

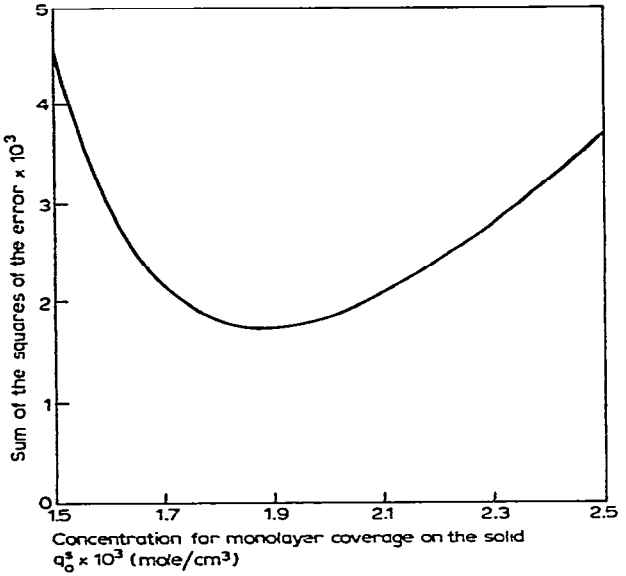

Fig. 2. The sum of the squares of the errors in the linear least-squares calculation *versus* the assumed concentration q_0^* for a monolayer coverage on the solid. For each q_0^*, the parameters v and K_m are calculated based on eqn. 14 and applied to calculate the error for the datum of an individual run.

Although eqn. 14 represents experimental data very well, we do not claim the superiority of this isotherm over others because data are needed over a wider range of concentrations and temperatures to support an isotherm. Also, the Chakravarti–Dhar isotherm is more applicable to chemisorption rather than to physical sorption[17]. These two adsorptions can be distinguished from their isosteric heats of adsorption which can be calculated from isotherm data at different temperatures. We are still conducting measurements at different temperatures; but the use of eqn. 13 is sufficient for this work.

Asymptotic concentration profile

Eqn. 9 is the general formula of the asymptotic concentration profile. The integral in eqn. 9 can be rewritten as

$$\frac{t_2 - t_1}{\tau} = \int_{C_1/C_0}^{C_2/C_0} \frac{dC/C_0}{\left(\frac{C}{C_0}\right)^v \left[\frac{1 + B^v}{1 + B\left(\frac{C}{C_0}\right)^v}\right] - \frac{C}{C_0}} \tag{15}$$

where

$$B \equiv K_m C_0. \tag{16}$$

Even though a numerical calculation is required, the application of eqn. 15 is not difficult because it includes only one parameter B, which can be determined from an isotherm. Actually, if one assumes that the asymptotic concentration profile has developed, then one can obtain an isotherm (up to the input concentration) from data of a single run without having any *a priori* knowledge of the isotherm[18]. A similar conclusion was reached in the study of GLC where both a very long column and a very long propagation time are usually achieved[19,20]. In the next section, we discuss criteria for an asymptotic concentration profile.

With the knowledge of K_m and B values, the transmission of the adsorbate can be determined (within an integration constant) from eqn. 15. The only unknown parameter is τ. Specifically, for each run with known flow-rate and other physical data, the parameter τ depends on the diffusion coefficient. Determination of the diffusion coefficient separately from the isotherm avoids fitting data with excessive parameters. In Table III, we list average values of τ for each run. These numbers were determined by using two successive transmissions between 0.1 and 0.9 for evaluating the integral in eqn. 15. Note that large errors in τ would result from using transmissions near zero or unity. The time constants are then determined from eqn. 15.

TABLE III

TIME CONSTANT, LONGITUDINAL DIFFUSION COEFFICIENT, HETP AND DIMENSIONLESS PARAMETERS α AND β FOR EACH RUN

Run No.	*Time constant, τ (sec)*	*Longitudinal diffusion coefficient, D (cm^2/sec)*	*HETP, H (cm)*	*Dimensionless parameters*	
				α	β
1	36	0.24	0.32	0.028	0.14
2	36	0.21	0.28	0.034	0.17
3	30	0.20	0.22	0.042	0.20
4	23	0.21	0.19	0.049	0.23
5A	43	0.16	0.22	0.063	0.34
5C	22	0.24	0.19	0.058	0.29
5C	11	0.38	0.17	0.054	0.25
6	22	0.23	0.18	0.061	0.30
7	22	0.26	0.19	0.064	0.34
8	20	0.28	0.18	0.064	0.35

Fig. 3 is a plot of the transmission *versus* $(t - t_{1/2})/\tau$ for runs 1, 3, and 5B. Since the half-transmission point always corresponds to zero on the abscissa, the time constant τ is the only adjustable parameter for fitting the data. A comparison in Fig. 3 reveals that the fitting is very good for high concentrations even at both ends. For lower concentrations with a more diffuse theoretical curve, the fit becomes poorer; furthermore, the measured concentration is higher than the theoretical results. This fact indicates that the gas-phase concentration is higher than the equilibrium values. The higher concentration is possible because of a mass-transfer resistance, or because the profile has insufficient time to diffuse completely.

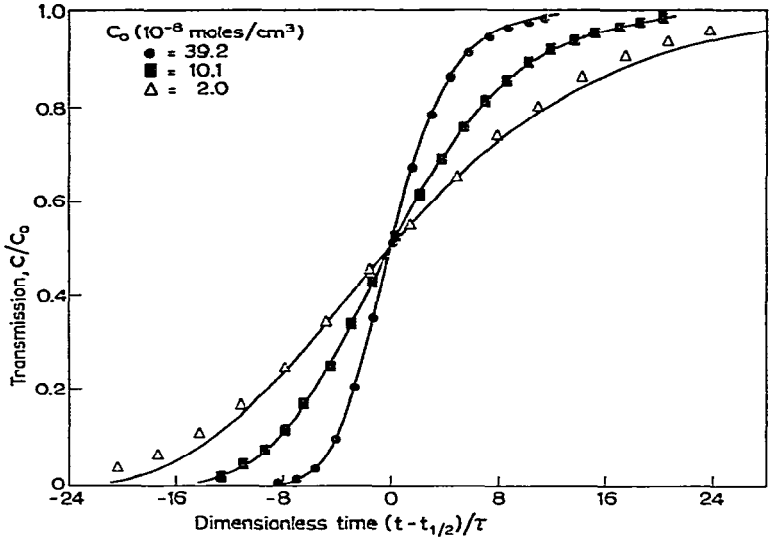

Fig. 3. The transmission *versus* the dimensionless time for runs 1, 3 and 5B.

Effect of flow-rate on transmission

To explore the possibility of non-equilibrium between gas and solid-phases, we varied the flow-rate for a fixed input concentration. For a given value of the input concentration C_0, the transmission data for different flow-rates can be superimposed on the same asymptotic concentration profile, as can be seen from eqn. 15. We measured the transmission of a 495 ppm mixture at three different flow-rates and plotted the results in Fig. 4. It can be seen that deviations exist for all runs, and that

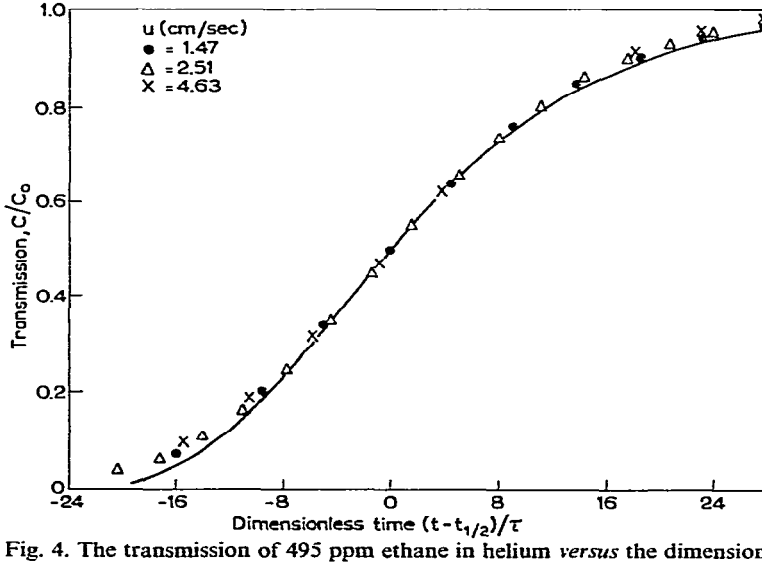

Fig. 4. The transmission of 495 ppm ethane in helium *versus* the dimensionless time for three flow-rates. The superficial flow velocities are 1.47, 2.51 and 4.63 cm/sec.

the deviations increase with the increasing flow-rate; however, the variations from one run to another are much smaller than the deviation from the theoretical results. This latter result indicates that the deviations in Figs. 3 and 4 are related to the applicability of eqn. 15 to low-concentration mixtures rather than to the effect of flow-rate.

The constant τ and the longitudinal diffusion coefficient D can be applied also to examine the effect of flow-rate on the transmission. Usually a high flow-rate will produce a steep transmission curve. In order to be able to superimpose data of the same input concentration (*e.g.*, runs 5A, 5B, and 5C) on a dimensionless time scale (in units of the time constant τ), the time constant τ must decrease with increasing flow-rate. The effect of diffusion in a chromatographic column is usually characterized by H, the height equivalent to a theoretical plate (HETP), which is defined as

$$H = \frac{2D}{u} \tag{17}$$

The relation between H and flow-rate is well-known in the literature[20]. The value of H first decreases sharply when the flow-rate increases and then increases gradually. The flow-rate dependences of H and D are shown in Fig. 5; the diffusion coefficient increases rapidly while H decreases. The decrease in H results from the combined effect of both flow-rate and longitudinal diffusion, but the effect of diffusion seems overwhelming. Although there is scatter in the values of the diffusion coefficients, they are roughly constant at low flow-rates and increase at high flow-rates. The constancy of the longitudinal diffusion coefficient at low flow-rates occurs because molecular diffusion dominates. Molecular diffusion is independent of flow-rate.

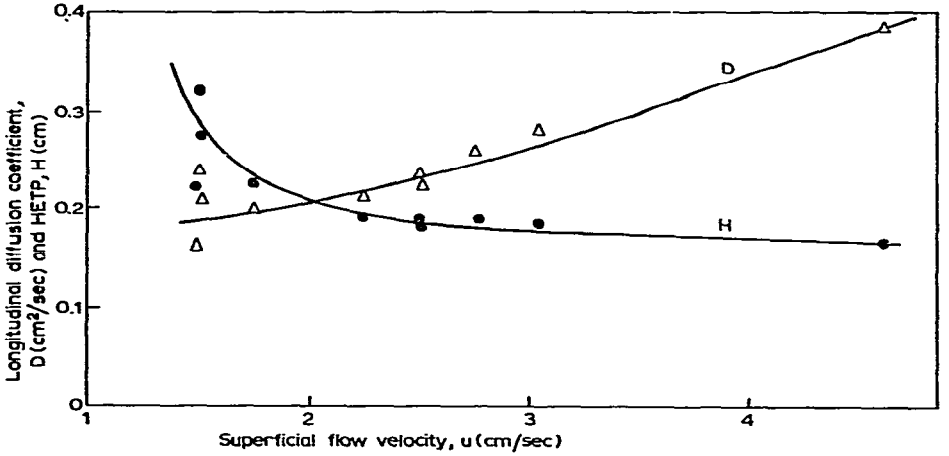

Fig. 5. The longitudinal diffusion coefficient and the HETP *versus* the superficial flow velocity. The solid lines are drawn to guide the eye.

At high flow-rates, the mass-transfer resistance between the gas-phase and the solid-phase causes a slow response for the solid-phase concentration which results in a wider concentration profile; consequently, the longitudinal diffusion coefficient in-

creases with flow-rate. The non-uniformity of the carrier gas flow in the radial direction of the chromatographic column also causes the longitudinal diffusion coefficient to increase with flow-rate. Since we saw that the comparison between the data and the theoretical curve is good for high-concentration mixtures and that the value of H is decreasing, it is concluded that the mass-transfer resistance is not the factor that causes the deviations in Fig. 3. Another factor, the speed of attaining an asymptotic profile, must be taken into consideration.

Analytic criteria for asymptotic concentration profiles

In order to achieve an asymptotic concentration profile, the adsorber must retain the adsorbate for a time long enough to develop the shape of the asymptotic profile. One expects a small flow-rate to result in a longer retention time and ease the development; however, a low flow-rate leads to a low diffusion coefficient which slows down the speed for development. Also, eqn. 9 points out that the asymptotic profile cannot be achieved for a linear isotherm in a finite time. The development of a concentration profile depends also on the curvature of the isotherm. The criterion for an asymptotic profile must involve a combination of these physical properties. From eqn. 8, one has

$$\frac{\hat{c}C}{\hat{c}Z} = \frac{u}{D} \frac{(Cq_0 - qC_0)}{\frac{\varepsilon C_0}{1-\varepsilon} + q_0} \tag{18}$$

which is the slope of the theoretical transmission curve with respect to the column coordinate Z. The characteristic width W for the adsorption profile to be eluted completely can be measured from the reciprocal slope evaluated at $C = C_0/2$.

$$\text{Characteristic width } W = -\Delta C \left(\frac{\hat{c}Z}{\hat{c}C}\right)_{C=C_0/2} \tag{19}$$

Letting $\Delta C = C_0$ for a step change in the adsorbate concentration, we have

$$W = \frac{DC_0}{u} \left. \frac{\frac{\varepsilon}{1-\varepsilon} C_0 + q_0}{(qC_0 - Cq_0)} \right|_{C=C_0/2} \tag{20}$$

The characteristic width W must satisfy two conditions for achieving an asymptotic profile: (1) the characteristic diffusion length δ must be larger than W so that the profile has enough time to develop; and (2) the column length L must be larger than W so that the end effect can be neglected.

During the elution time, Brownian motion diffuses the front of the profile; the characteristic diffusion length δ for the Brownian motion during a time t_p is

$$\delta \approx (Dt_p)^{1/2} \tag{21}$$

Based on the first condition, an analytical criterion for an asymptotic profile is

$$1 \gg \frac{W}{\delta} = \left(\frac{D}{uL}\right)^{1/2} \left| \frac{\left(\frac{\varepsilon}{1-\varepsilon} + K_0\right)}{\left(\frac{q}{C_0} - \frac{C}{C_0} K_0\right)\left(1 + \frac{K_0 (1-\varepsilon)}{\varepsilon}\right)^{1/2}} \right|_{C=C_0/2} \tag{22}$$

or, approximately

$$1 \gg \frac{W}{\delta} \approx \left(\frac{D}{uL}\right)^{1/2} \frac{2K_0^{1/2}}{K_{1/2} - K_0} \equiv \alpha \tag{23}$$

where $K_{1/2}$ is the dimensionless adsorption capacity at $C = C_0/2$. Eqn. 23 is valid in the approximation that $K_0 \gg \frac{\varepsilon}{1-\varepsilon} \approx 1$. Both K_0 and $K_{1/2}$ are calculated from eqn. 13.

The second condition for W is expressed as

$$1 \gg \frac{W}{L} = \frac{D}{uL} \left| \frac{\left(\frac{\varepsilon}{1-\varepsilon} + K_0\right)}{\left(\frac{q}{C_0} - \frac{C}{C_0} K_0\right)} \right|_{C=C_0/2} \tag{24}$$

or, approximately

$$1 \gg \frac{W}{L} \approx \left(\frac{D}{uL}\right) \frac{2K_0}{K_{1/2} - K_0} \equiv \beta \tag{25}$$

Eqn. 25 is valid in the same approximation leading to eqn. 23.

Both eqns. 23 and 25 indicate that the asymptotic profile is very sensitive to the curvature of the isotherm. For a linear isotherm, the adsorption capacity is constant ($K_{1/2} = K_0$); thus, the inequality is never satisfied. The ratio of the adsorption capacities in eqns. 23 and 25 dominates the values of α and β. In Table III we list values of α and β. Because of the square-root dependences in eqn. 23, the variation of α is smaller than the variation of β within our experimental conditions. Since the value of α is smaller than β even after considering the factor $\varepsilon/(1-\varepsilon)$, β is the stronger criterion. The inequality for β is best satisfied for the highest concentrations; however, for low concentrations, the increase in the value of β causes the inequality to be less well satisfied and accounts for the deviation between experiment and theory.

Eqns. 23 and 25 also point out that for the same concentration, the criteria decrease with D/u. Since D/u happens to have the same functional relation as H, we expect that the minimum of H gives the best fit to the theoretical curve. This result agrees with common practice in gas-chromatograph analysis where the minimum of H gives the narrowest peak and the best separation[20].

The combination of the effects of flow-rate and curvature also explains why the low-concentration mixture cannot give a good asymptotic profile. The β values for

495-ppm mixtures are higher than that for the 9830-ppm or the 2478-ppm mixtures. Increasing the flow-rate from 1.47 to 2.51 cm/sec decreased β from 0.34 to 0.29 for the 495-ppm mixture. A further increase of flow-rate to 4.63 cm/sec decreased β to 0.25. Since there is a minimum in the flow-velocity dependence of H, a further increase in the flow-rate would increase β again. The only possibility for achieving the asymptotic profile is to increase the column length L, which has no limitation. The comparison of β values does not explain why the result of run 5C, which has the lowest β value, is the worst among the three runs for the 495-ppm mixture; the reason may be that the mass-transfer resistance inside the carbon granules becomes relatively important at high flow-rates.

CONCLUSION

We measured the transmission of ethane in a helium carrier-gas flow for ethane compositions between 50 and 10,000 ppm on activated carbon; derived the adsorption isotherm of ethane at 25°C; and incorporated the adsorption isotherm into an asymptotic concentration profile formula. It is found that the transmission of high concentrations agrees with theory and that for low concentrations is higher than theory. Analytical expressions are suggested as the criteria for an asymptotic profile. We concluded that an asymptotic profile is easy to achieve with a high flow-rate, a long column length, a low diffusion coefficient, and a large curvature for the isotherm; however, the criteria cannot explain the small differences between results of different flow-rates for the same concentration. Further investigation may be warranted on the effect of the mass-transfer resistance on the asymptotic concentration profile.

ACKNOWLEDGEMENT

This work was supported in part by the U.S. Department of Energy.

REFERENCES

1 A. V. Kiseler and Y. Z. Yashin, *Gas-Adsorption Chromatography*, Plenum, New York, 1969.
2 R. Aris and N. R. Amundson, *Mathematical Methods in Chemical Engineering*, Vol. 2, Prentice-Hall, Englewood Cliffs, NJ, 1973.
3 R. Courant and D. Hilbert, *Methods of Mathematical Physics*, Vol. 2, Wiley-Interscience, New York, 1962.
4 L. Lapidus and N. R. Amundson, *J. Phys. Chem.*, 56 (1952) 948.
5 E. Gluckauf, *Trans. Faraday Soc.*, 51 (1955) 34.
6 L. G. Sillen and E. Ekedahl, *Ark. Kemi, Min. Geol.*, A22 (1946) 22.
7 L. Lapidus and J. B. Rosen, *Chem. Eng. Progr., Symp. Ser.*, 50, No. 14 (1954) 97.
8 E. N. Lightfoot, *J. Phys. Chem.*, 61 (1957) 1686.
9 A. Acrivos, *Chem. Eng. Sci.*, 13 (1960) 1.
10 K. B. Lee and R. Madey, *Trans. Faraday Soc.*, 67 (1971) 329.
11 J. C. Huang, R. Forsythe and R. Madey, *Separ. Sci. Technol.*, 16 (1981) 475.
12 D. R. Garg and D. M. Ruthven, *Chem. Eng. Sci.*, 30 (1975) 1192.
13 R. Forsythe, M. Czayka, R. Madey and J. Povlis, *Carbon*, 16 (1978) 27.
14 J. P. Hobson, in E. A. Flood (Editor), *The Solid–Gas Interface*, Vol. 1, Marcel Dekker, New York, 1966, pp. 447–489.
15 M. M. Dubinin, *Progr. Surface Membrane Sci.*, 9 (1975) 1.

16 D. N. Chakravarti and N. R. Dhar, *Kolloid.-Z.*, 43 (1907) 377.
17 K. J. Laidler, in P. H. Emmett (Editor), *Catalysis*, Vol. 2, Reinhold, New York, 1954.
18 D. deVault, *J. Amer. Chem. Soc.*, 65 (1943) 532.
19 J. R. Conder and J. H. Purnell, *Trans. Faraday Soc.*, 65 (1969) 824, 839.
20 R. J. Laub and R. L. Pecsok, *Physiochemical Applications of Gas Chromatography*, Wiley, New York, 1978.